Calculation of Thermophysical Properties of Carbon and Low Alloyed Steels for Modeling of Solidification Processes

JYRKI MIETTINEN and SEPPO LOUHENKILPI

Algorithms and a computer software package for calculating thermophysical material properties of carbon and low-alloyed steels, associated with the simulation of solidification processes, have been developed. The earlier studies on kinetic phase transformation modeling are applied and are the base of the present work. The calculation algorithms are based on thermodynamic theory connected to thermodynamic assessment data, as well as on regression formulas of experimental data, and they take into account the temperature, the cooling rate, and the steel composition. The calculation algorithms and some results of calculations are presented in this article.

I. INTRODUCTION

THE modeling of solidification systems is a problem of a great mathematical and industrial significance. In recent years, computer simulation models have been developed to simulate heat transfer in solidification processes. Numerical methods, mostly finite difference or finite element methods, are effectively used. However, to obtain reliable results, accurate data on the thermophysical material properties are also needed. Typical data needed are the density, the thermal conductivity, and the specific heat. Other important data are the phase transformation temperatures and the corresponding latent heats, and also the way in which the latent heats are released during the phase transformations. If so-called enthalpy formulation is used, the enthalpy values can directly be used if they are known. The enthalpy then includes all the other data except the thermal conductivity and the density.

The material data are not only functions of the temperature and the composition but also of the cooling rate. This is because the kinetics of phase transformations depend on the cooling rate and the thermophysical properties are related to the phases formed. At high temperatures, a high cooling rate typically lowers the phase transformation temperatures, especially the solidus temperature, but not drastically, due to the compensating effect of a finer dendritic microstructure. At low temperatures, however, the effect of the cooling rate upon the phase transformation temperatures is much clearer. Thus, for accurate simulation of solidification and cooling processes, one should be able to know the material data as a function of temperature, composition, and cooling rate.

Normally, the material data are taken from the literature. It is seldom possible, however, to find all the data needed. Although material data have been measured for a great number of steel grades, most of these data are valid for the low-temperature region only, and there are only few data for higher temperatures up to the liquid

phase. Moreover, these data are usually expressed as a function of temperature and composition only, i.e., the cooling rate is not taken into account. So, it is seldom possible to find all the data needed. This is especially the case for carbon and low-alloyed steel grades, because in these steels, even small variations in the composition may have a significant effect on the thermophysical material properties. A model that could simulate the thermophysical material properties of steels, taking into account the cooling and the composition, seems not to be available.

Therefore, algorithms and a computer software package for calculating thermophysical material properties of steels, taking into account the temperature, the cooling rate, and the composition, have been developed. The earlier studies on kinetic phase transformation modeling are applied, and they are the base of the present work.[1,2,3] The calculation algorithms are based on thermodynamic theory connected to thermodynamic assessment data and on regression formulas of experimental data. The package is now valid for carbon and low-alloyed steel grades and is under progress for stainless and alloyed steels. The calculation algorithms and some obtained results are presented in this article.

II. THERMAL MODELING OF SOLIDIFICATION

A general solidification phase change system without convection can be described by the following equation:

$$\rho c \frac{\partial T}{\partial t} = \frac{\partial}{\partial x}\left(k\frac{\partial T}{\partial x}\right) + Q \qquad [1]$$

Here, ρ is the density, c is the specific heat, k is the thermal conductivity, and Q is a term describing the rate of energy released by the phase transformations. For solidification phase change, it can be defined as

$$Q = \rho L \frac{\partial(f_s)}{\partial t} \qquad [2]$$

Here, L is the latent heat of the solidification, and $f_s = f_s(T)$ is called the solidified fraction in the mushy zone. The later term describes the way in which the latent heat

JYRKI MIETTINEN, Research Engineer, and SEPPO LOUHENKILPI, Senior Teaching Assistant, are with the Laboratory of Metallurgy, Helsinki, University of Technology, 02150 Espoo, Finland.

is released during solidification. This way depends strongly on the chemical composition of the material to be cast. The solid-state phase transformations can be treated in a similar way. Therefore, the material data needed are the density, the specific heat, the thermal conductivity, the latent heats, and the phase fractions during the phase transformations.

Equation [1] also can be expressed in another form by using so-called enthalpy formulation. The enthalpy, H, is defined as the sum of the sensible ($\int C_p \cdot dT$) and the latent heats. Equation [1] now becomes

$$\rho \frac{\partial H}{\partial t} = \frac{\partial}{\partial x}\left(k \frac{\partial T}{\partial x}\right) \qquad [3]$$

In this case, the necessary material data are the density, the enthalpy, and the thermal conductivity. The enthalpy now includes all the other material data, except the density and the thermal conductivity. Hence, the enthalpy values can directly be used if they are known.

In the heat-transfer models, it is usually assumed that the material data are functions of the temperature and the composition only. The cooling rate, however, is also an important parameter, because it affects phase transformations and therefore the thermophysical material properties. Normally, the cooling rate varies at different distances from the casting surfaces and also in time. To be precise, this should be taken into account when solving the heat-transfer equations. So, for accurate simulation of solidification processes, one should be able to know or model the material data as a function of temperature, composition, and cooling rate, and this model or knowledge should then be coupled in a proper way to the heat-transfer calculations.

Equation [1] or [3] is normally solved using fixed grids. This means that the contraction of the steel is not calculated and taken into account, i.e., the density cannot be varied either. In such cases, the density should be that of the initial liquid and constant. However, during solidification, the fluid in interdendritic space is free to move, and it more or less compensates the so-lidification contractions. To take this feeding into account, the density for the solid phase should be the density at the solidus temperature, while above the solidus, the density should vary as a function of temperature.

III. CALCULATION OF THERMOPHYSICAL PROPERTIES

Depending on composition, the solidifying steel goes through some of the following phase transformations: L → δ, L → γ, L + δ → γ, and δ → γ, where L denotes liquid, δ denotes delta ferrite, and γ denotes austenite. In order to simulate these transformations in carbon and low-alloyed steels, an interdendritic solidification model (IDS), was developed.[1,2] In this model, the main instruments of conventional solute redistribution models (i.e., material balance equations and Fick's diffusion laws) are coupled to a thermodynamic solution model, which relates the compositions of the phase interfaces to temperature and the phase stabilities. The calculations

are made in one volume element placed on the side of a dendrite arm (Figure 1), assuming a complete mixing in the liquid phase. As a result, one obtains the phase fractions $f^\phi(\phi = L, \delta, \gamma)$ and the phase compositions X_i^ϕ ($i = 1, ..., n$; $\phi = L, \delta, \gamma$) as a function of temperature within the range 1000 °C to 1600 °C (here, n is the number of components in the alloy). These results, of course, depend on the cooling rate of the process and the chemical analysis of the alloy. Note that the cooling rate, given as input data, does not need to be constant. Normally, the cooling rate varies at different distances from the casting surfaces and also in time. This can now be taken into account. Note also that as the model deals with nonequilibrium solidification, X_i^ϕ will vary in ferrite and austenite. Consequently, inside these phases, special concentration profiles will be formed (in liquid, this will not happen due to the complete mixing).

At lower temperatures ($T < 1000$ °C), austenite can decompose via the following phase transformations: $\gamma \rightarrow p\alpha$, $\gamma \rightarrow pc$, and $\gamma \rightarrow e\alpha + ec$, where $p\alpha$ denotes pro-eutectoid ferrite, pc denotes proeutectoid cementite, and $e\alpha + ec$ denotes a mixture of eutectoid ferrite and cementite, called pearlite or bainite. In addition, during rapid cooling, austenite may transform at low temperatures to carbon-saturated ferrite (martensite) as $\gamma \rightarrow m\alpha$. In order to simulate these transformations in carbon and low-alloyed steels, a semiempirical austenite decomposition model (ADC)[3] was developed. Here, empirical formulas based on continuous cooling transformation (CCT) experiments were evaluated to predict the temperature ranges of different structures (γ, $p\alpha$, pc, $e\alpha + ec$, $m\alpha$) as a function of alloy composition, cooling rate, and austenite grain size. These formulas were then coupled to a thermodynamic model, assuming a paraequilibrium condition during the phase transformations. This means that only carbon distributes between different phases, whereas the other components tend to inherit the composition of austenite in all phases. As a result of the calculations, one obtains the fractions of the structures, f^ϕ ($\phi = \gamma$, $p\alpha$, pc, $e\alpha + ec$, $m\alpha$), and the phase compositions, X_i^ϕ ($i = 1, ..., n$), as functions of temperature within the range $T = 25$ °C to 1000 °C. Note that the cooling rate must be constant in the ADC model. The reheating or varying cooling rate cannot be taken into account. Another problem is the determination of the original austenite grain size after solidification. Accurate data seem not to be available. This item will be studied more precisely in the future. The IDS
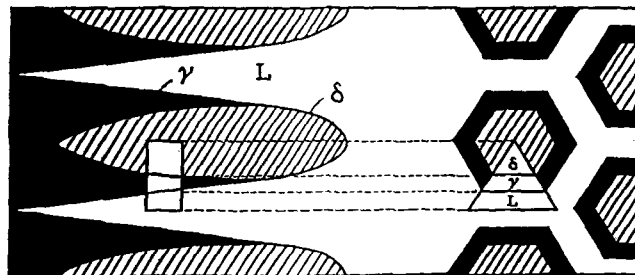

Fig. 1—Longitudinal and transverse cross section of dendrites with a volume element on the side of a dendrite arm.

and ADC models are now valid for carbon and low alloyed steels.

When evaluating thermophysical properties for an alloy, one has to know the properties of the individual phases and the fractions of these phases. In the case of steels, the phase fractions can be calculated with the IDS and the ADC models as shown previously. Assuming now that the thermophysical properties are the same for all ferritic phases (δ, $p\alpha$, $e\alpha$, $m\alpha$) and for both cementite phases (pc, ec), the evaluation procedure can be simplified considerably. This implies, however, that the total fractions of ferrite and cementite expressed as

$$f^\alpha = f^\delta + f^{p\alpha} + f^{e\alpha} + f^{m\alpha} \qquad [4]$$

$$f^c = f^{pc} + f^{ec} \qquad [5]$$

are known. Here, terms $f^\delta, f^{p\alpha}, f^{m\alpha}$, and f^{pc} can be calculated directly with the IDS and the ADC models, and terms $f^{e\alpha}$, and f^{ec} can be approximated from the binary Fe-C phase diagram as

$$f^{ea} \approx \frac{(6.69 - \text{pct C})}{6.69} \cdot f^{ea+ec} \qquad [6]$$

$$f^{ec} \approx \frac{\text{pct C}}{6.69} \cdot f^{ea+ec} \qquad [7]$$

where pct C is the carbon content in weight percent and f^{ea+ec} is the fraction of pearlite or bainite (or their mixture) calculated with the ADC model. Therefore, knowing the fractions and the thermophysical properties of liquid, ferrite, austenite, and cementite, one is able to evaluate the properties for the whole steel from room temperature up to liquid phase. In Sections III–A through C, special formulas are given to calculate molar enthalpy, molar specific heat, thermal conductivity, and density for carbon and low-alloyed steels.

A. Calculation of Enthalpy and Enthalpy-Related Data as Specific and Latent Heats

According to classical thermodynamics, the molar enthalpy H and the molar specific heat C_p of a system can be expressed as

$$H = G - T\left(\frac{dG}{dT}\right)_p \qquad [8]$$

$$C_p = -T\left(\frac{d^2G}{dT^2}\right)_p \qquad [9]$$

where G is the molar Gibbs energy of the system. For a heterogeneous phase mixture containing π phases, the molar Gibbs energy can be given as

$$G = \sum_{k=1}^{\pi} f^{\phi k} G^{\phi k} \qquad [10]$$

where $f^{\phi k}$ is the fraction of phase ϕk and $G^{\phi k}$ is the molar Gibbs energy of that phase. For carbon and low-alloyed steels, Eq. [10] can be written as

$$G = f^l G^l + f^\alpha G^\alpha + f^\gamma G^\gamma + f^c G^c \qquad [11]$$

In Eq. [11], term G^ϕ for liquid, ferrite, and austenite can be expressed as

$$G^\phi = \sum_{i=1}^{n} X_i^\phi \mu_i^\phi \qquad [12]$$

Here, n is the number of components in the alloy, X_i^ϕ is the mole fraction of component i in phase ϕ, and μ_i^ϕ is the chemical potential of the component i in that phase. A precise description of the chemical potential depends on the solution model to be used. In this study, the Wagner–Lupis–Elliott model (WLE)[4,5,6] was chosen because it can be well applied to the dilute solution phases of carbon and low-alloyed steels.[2] In addition, the model is simple and its database can be easily extended with special data-conversion formulas.[2] When applying the WLE model to the phases of iron-base alloys ($\phi = L, \alpha, \gamma$), the chemical potentials of iron and solute elements can be expressed as

$$\mu_{Fe}^\phi = (G_{Fe}^{0\alpha} - H_{Fe}^{SER}) + (G_{Fe}^{0\phi} - G_{Fe}^{0\alpha})$$
$$+ RT \ln X_{Fe}^\phi + G_{Fe}^{E\phi} \qquad [13]$$

$$\mu_i^\phi = (G_i^{0\theta} - H_i^{SER}) + (G_i^{0\phi} - G_i^{0\theta})$$
$$+ (G_i^{\infty\phi} - G_i^{0\phi}) + RT \ln X_i^\phi + G_i^{E\phi} \qquad [14]$$

By means of the terms $G_i^{0\theta} - H_i^{SER}$ and $G_i^{0\phi} - G_i^{0\theta}$ (here, i also stands for iron), the Gibbs energy of phase ϕ is expressed relative to a special reference state (SER),[7] i.e., the enthalpies of pure elements in their defined reference phase at 298.15 K and 10^5 Pa. For iron, the reference phase is α and for solute elements, it is described by θ in Eq. [14]. The third term in Eq. [14], $G_i^{0\phi} - G_i^{0\phi}$, changes the reference state of solute elements in phase ϕ from that of pure elements (Raoultian standard state) to the state of infinite dilution (Henrian standard state), in regard to which the effect rising from randomly mixed atoms (term $RT \ln X_i^\phi$) and solutal interactions (term $G_i^{E\phi}$) will be expressed. The last term, the partial excess Gibbs energy $G_i^{E\phi}$, is given for iron and the solute elements ($i = 2, \ldots, n$) as follows:[2,7]

$$G_{Fe}^E = A \cdot \sum_{i=2}^{n} \sum_{j=2}^{n} RT\varepsilon_i^j X_i X_j + 2B$$
$$\cdot \left[\sum_{i=2}^{n} RT\rho_i^i X_i^3 + \sum_{i=2}^{n} \sum_{j=2}^{n} \sum_{\substack{k=2 \\ k \neq i}}^{n} RT\rho_i^{jk} X_i X_j X_k \right] \qquad [15]$$

$$G_i^E = \sum_{j=2}^{n} RT\varepsilon_i^j X_j + \sum_{j=2}^{n} RT\rho_i^j X_j^2$$
$$+ \sum_{j=2}^{n} \sum_{k>j}^{n} RT\rho_i^{jk} X_j X_k \qquad [16]$$

where

$$A = \left[\ln\left(1 - \sum_{i=2}^{n} X_i\right) + \sum_{i=2}^{n} X_i \right] \bigg/ \left(\sum_{i=2}^{n} X_i\right)^2 \qquad [17]$$

$$B = \left[\ln\left(1 - \sum_{i=2}^{n} X_i\right) + \sum_{i=2}^{n} X_i \right.$$

$$\left. + \frac{1}{2}\left(\sum_{i=2}^{n} X_i\right)^2 \right] \bigg/ \left(\sum_{i=2}^{n} X_i\right)^3 \qquad [18]$$

Here, parameters ε_i^j, ρ_i^j, and ρ_i^{jk} describe chemical interactions between different solutes (the phase symbol ϕ has been omitted for the sake of clarity).

By ignoring the interactions between the substitutional solutes in cementite, term G^c for cementite in Eq. [11] can be approximated as

$$G^c = \frac{1}{4} \cdot \left[\sum_{M=1,M\neq 1}^{n} Y_M^c(G_{M_3C}^{0c} - 3H_M^{SER} - H_C^{SER}) \right.$$

$$\left. + 3RT \sum_{M=1,M\neq 2}^{n} Y_M^c \ln Y_M^c + \sum_{M=3}^{n} Y_{Fe}^c Y_M^c L_{FeM}^c \right] \qquad [19]$$

Here, Y_M^c is the site fraction of substitutional element M occupying sublattice (Fe, M) in cementite $(Fe, M)_3C$. The term $G_{M_3C}^{0c}$ is the Gibbs energy of pure compound M_3C, and L_{FeM}^c is a parameter describing the interaction of Fe and M in sublattice (Fe, M). Note that carbon C designated as 2 occupies another sublattice. By means of the terms $(G_{M_3C}^{0c} - 3H_M^{SER} - H_C^{SER})$, the Gibbs energies of pure compounds M_3C are expressed relative to the reference state SER.

Values for terms $G_i^{0\theta} - H_i^{SER}$ and $G_i^{0\phi} - G_i^{0\theta}$ in Eqs. [13] and [14] have been given by Dinsdale,[7] and values for terms $G_{M_3C}^{0c} - 3H_M^{SER} - H_C^{SER}$ and L_{FeM}^c have been given by Huang[8] and Qiu.[9] In addition, special data-conversion formulas have been derived[2] to evaluate values for terms $G_i^{\alpha\phi} - G_i^{0\phi}$ and the interaction parameters of Eqs. [13] and [14]. It should be remembered that the published or the evaluated values of all the thermodynamic parameters discussed previously are finally based on experimental measurements such as activity measurements, such as activity measurements, heat-capacity and mixing-enthalpy measurements, and gas equilibrium and solubility data.

When applying Eq. [11], the ferritic term $f^\alpha G^\alpha$ should be expressed as $f^\alpha G^\alpha = f^\delta G^\delta + f^{p\alpha} G^{p\alpha} + f^{e\alpha} G^{e\alpha} + f^{m\alpha} G^{m\alpha}$ because the composition in the ferritic phases is not the same. The thermodynamic data of ferrite, however, are the same for all the terms G^δ, $G^{p\alpha}$, $G^{e\alpha}$, and $G^{m\alpha}$. In the case of cementite, one may apply $G^c = G^{pc} = G^{ec}$ due to the paraequilibrium condition assumed. Finally, it should be remembered that when applying the equations of this section to calculate the molar enthalpy or the molar specific heat of the alloy, the mole fraction X_i^ϕ in the equations refers to the average composition in the phase. This can be estimated from the concentration profiles obtained with the IDS or the ADC model.

Now, knowing H and Cp by means of Eqs. [8] and [9], one can then approximate the latent heat of solidification (L) from Eq. [20] as

$$L = \Delta H_{T_s \to T_l} - \int_{T_s}^{T_l} C_p \cdot dT \qquad [20]$$

where T_l and T_s are the liquidus and the solidus temperatures of the alloy. The latent heats of solid state phase transformations can be calculated in a similar way. The specific heat and the latent heats are enthalpy-related data, and as mentioned previously, when using the so-called enthalpy formulation (Eq. [3]), enthalpy values can be used directly as input data in the heat-transfer models. In this case, the specific heat and the latent heats need not be calculated.

B. Calculation of Thermal Conductivity

In carbon and low-alloyed steels, thermal conductivity is usually not known for each individual solid phase but rather for the solid state only. In this case, it is reasonable to treat the solid phases as a one phase and apply only two-phase fractions, f^l (liquid fraction) and f^s (solid fraction), in calculations. Knowing that the solid fraction can be expressed as $f^s = 1 - f^l$, the thermal conductivity of the alloy can be calculated with equation

$$k = (1 - f^l)k^s + (1 + A_{mix})f^l k^l \qquad [21]$$

Here, k^s and k^l are the thermal conductivities in solid and liquid state and A_{mix} is a parameter describing the effect of liquid convection upon the thermal conductivity. If the constant A_{mix} is 0, there is no increased heat transfer in the mushy or liquid regions due to convection, i.e., the liquid phase is stagnant. This technique, called effective thermal conductivity, is most often used to account for the convective heat transfer in the liquid during solidification.[10–13] The value of A_{mix} depends on the mixing intensity, and it can be determined experimentally. For a continuous-steel-casting process, for instance, a value of $A_{mix} = 4$ to 6 may be applied.[10–13]

Thermal conductivity has been measured in many carbon and low-alloyed steels at low temperatures,[14–17] but at higher temperatures up to the liquidus temperature, only a few measurements are available.[14,16,17]

In this work, the thermal conductivity in liquid is assumed to have a constant value of

$$k^l = 35 \quad \left(\frac{W}{Km}\right) \qquad [22]$$

This value, representing the thermal conductivity of pure iron at T_l, was chosen because of the lack of data for liquid steels. In addition, above the A_3 temperature, the influence of alloying upon the thermal conductivity is known to be small.[17]

In the solid, the thermal conductivity is evaluated by applying a linear regression analysis to the experimental measurements.[14,15,16] As a result of the analysis, four formulas of the type

$$k^s = k_0 + \Sigma a_i C_i \quad \left(\frac{W}{Km}\right) \qquad [23]$$

were obtained corresponding to temperatures 1000 °C, 400 °C, 200 °C, and 25 °C, as shown in Table I. In these formulas, a_i represents the effect of solute i upon k^s, and C_i is the composition of solute i. As can be seen, the correlation coefficients are quite high.

Assuming that $k^s = k^l$ at the liquidus temperature, Eq. [22] and the formulas of Table I can be used to interpolate a value for k^s at any temperature. At temperatures

Table I. Thermal Conductivity $k^s = k_0 + \Sigma a_i C_i$ in Low-Alloyed Steels at Different Temperatures*

T (°C)	k_0	a_C	a_{Si}	a_{Mn}	a_{Cr}	a_{Mo}	a_{Ni}	a_V	N	r
1000	28.12	−1.60	−0.18	−0.55	—	—	—	—	9	0.93
400	47.70	−7.70	−5.12	−3.37	−3.10	0.59	−1.68	−6.07	71	0.93
200	57.56	−9.98	−8.85	−6.65	−5.00	−0.48	−3.12	−8.84	73	0.94
25	68.15	−15.9	−12.4	−12.5	−7.87	−1.71	−4.61	−9.99	66	0.95

*The value of k is given in W/Km and C is given in Weight Percent, N = number of alloys, and r = correlation coefficient.

$T < 1000$ °C, however, the interpolation should be made with the k^s/T slope of the previous temperature range until proeutectoid ferrite, proeutectoid cementite, or pearlite begins to form at $T = T'$ (Figure 2). After this, the interpolation should be made between $T = T'$ and $T = 400$ °C by applying the proper k^s values of these temperatures.

C. Calculation of Density

In general, the density of a heterogeneous phase mixture containing π phases can be defined as[18]

$$\rho = 1 \bigg/ \sum_{k=1}^{\pi} f^{\phi k}/\rho^{\phi k} \qquad [24]$$

where $f^{\phi\kappa}$ is the fraction of phase ϕk and $\rho^{\phi\kappa}$ is the density of that phase. In the case of carbon and low-alloyed steels, Eq. [24] can be expressed as

$$\rho = 1 \bigg/ \left[\frac{f^l}{\rho^l} + \frac{f^\alpha}{\rho^\alpha} + \frac{f^\gamma}{\rho^\gamma} + \frac{f^c}{\rho^c}\right] \qquad [25]$$

where f^a and f^c are given by Eqs. [4] and [5]. At high temperatures ($T > 1000$ °C), terms f^l, f^δ, and f^γ, are calculated with the IDS model and the other f^ϕ terms are set to zero, whereas at low temperatures, terms f^l and f^δ are set to zero and the other f^ϕ terms are calculated with the ADC model, applying Eqs. [6] and [7].
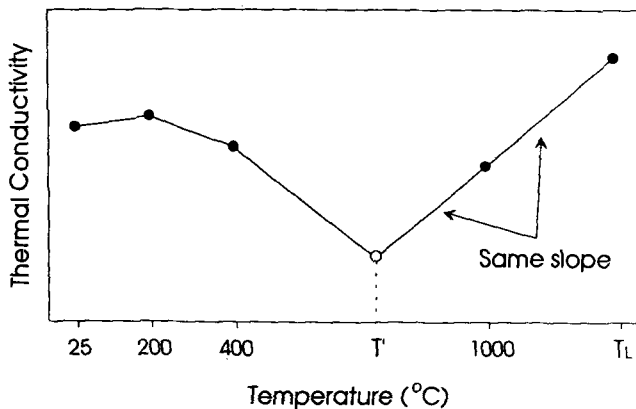

Fig. 2—Schematic view on interpolation of thermal conductivity k^s below the liquidus temperature (T_l) by applying known k^s values of certain temperatures (black spots). The white spot refers to the formation of proeutectoid ferrite, proeutectoid cementite, or pearlite at temperature T'.

In Eq. [25], the density of liquid, ferrite, austenite, and cementite can be calculated from the equations

$$\rho^l = (8319.49 - 0.835 \cdot T)$$
$$\cdot (1 - 0.01 \cdot \text{pct C}) + A^L \qquad [26]$$

$$\rho^\alpha = (7875.96 - 0.297 \cdot T - 5.62 \cdot 10^{-5} \cdot T^2)$$
$$\cdot (1 - 0.0246 \cdot \text{pct C}) + A^S \qquad [27]$$

$$\rho^\gamma = (8099.79 - 0.506 \cdot T)$$
$$\cdot (1 - 0.0146 \cdot \text{pct C}) + A^S \qquad [28]$$

$$\rho^c = 7686.45 - 0.0663 \cdot T - 3.12 \cdot 10^{-4} \cdot T^2 \qquad [29]$$

where

$$A^L = -67.5 \text{ pct Si} - 3.9 \text{ pct Mn} - 8.6 \text{ pct Cr}$$
$$+ 24 \text{ pct Mo} + 3.3 \text{ pct Ni} \qquad [30]$$

$$A^S = -63.1 \text{ pct Si} - 6.1 \text{ pct Mn} - 9.3 \text{ pct Cr}$$
$$+ 2.6 \text{ pct Mo} - 0.3 \text{ pct Ni} \qquad [31]$$

Here, density ρ is given in kg/m^3, temperature T is given in °C, and solute contents are given in weight percent. These sentences, excluding terms A^L and A^S, are based on the analysis of Jablonka et al.[18] for pure iron and iron-carbon alloys. The term A^L was evaluated from the density measurements for liquid binary iron alloys,[19,20] and the term A^S was calculated by applying a linear regression analysis to the density measurements given for multicomponent steels at the room temperature.[16] The regression analysis included 30 alloys and yielded the value 0.987 for the correlation coefficient. In the analysis, carbon was not included as a regression variable, but its effect was taken into account by applying the following formulation:

$$\rho^{\text{measured}} = 6.69 \bigg/ \left[\frac{6.69 - \text{pct C}}{\rho^\alpha} + \frac{\text{pct C}}{\rho^c}\right]$$
$$+ \Sigma a_i C_i \qquad [32]$$

where the term $\Sigma a_i C_i$ equals the term A^S to be solved, and ρ^α and ρ^c were calculated from Eqs. [27] and [29] by setting $T = 25$ °C and $A^S = 0$. Hence, the A^S term describes the effect of solutes, excluding carbon, upon the density of ferrite at the room temperature. This term also is applied to austenite because of the lack of density measurements for that phase.

IV. EXAMPLES AND DISCUSSION

The IDS and ADC models calculate the temperature ranges of phase transformations, as well as the phase

fractions during the transformations. These models were tested by comparing the calculated results with numerous experimental values, and a reasonable correlation was found between the results.[1,2,3] The calculation of thermal conductivity is based on regression formulas of experimental data and, due to the high values of the correlation coefficients (Table I), the results should be quite reliable. At high temperatures, however, the data available are meager and their validity is difficult to estimate.

The calculation of density is based on the results of the IDS and ADC models and on experimental data. For pure iron and iron-carbon alloys, the experimental data were taken from the analysis of Jablonka et al.[18] They calculated the effect of carbon on the density in iron-carbon alloys as a function of temperature and found a good agreement between the calculated and measured results. In order to take other solute elements into account, regression formulas were evaluated. Enough data to make an acceptable regression were found, however, only at 25 °C and in the liquid range. Thus, one equation was evaluated for the liquid phase and one for 25 °C. The latter also is used over the range between 25 °C and the solidus temperature. The error is not necessarily significant, but one aim for the future work is to find more data for the density. On the other hand, when using fixed grids in the heat-transfer calculations, the contraction of the steel is not calculated and taken into account and so the density cannot be varied either (Section II).

The calculation of enthalpy and enthalpy-related data as specific and latent heats is based on the results of the IDS and ADC models, thermodynamic theory, and thermodynamic assessment data. The thermodynamic data bank of the models contains data for the following elements: Fe, Al, B, C, Ca, Cr, Cu, Mn, Mo, N, Nb, Ni, O, P, S, Si, Ti, and V. Because of the numerous thermodynamic assessments available today, especially for iron-base alloys, the thermodynamic calculations can from this point of view be considered quite reliable. An accurate comparison between calculated and measured results has been made for pure iron and the Fe-C system only. In both cases, an excellent agreement comparable to those in References 21 and 22 was obtained. For alloyed steel, only a few experimental data are available, and we are now searching for more data to do accurate comparisons.

Figures 3 through 6 show calculated results for pure iron and for two steel grades, which differ only in carbon content. The effect of the composition on the results clearly can be seen. For instance, in pure iron, the phase transformations take place at constant temperatures, whereas in steels within a certain temperature range. The phase transformations taking place are as follows:

for pure iron, $L \rightarrow \delta \rightarrow \gamma \rightarrow \rho\alpha$

for the 0.1 pct Csteel, $L \rightarrow \delta$, $L + \delta \rightarrow \gamma$, $\delta \rightarrow \gamma$, $\gamma \rightarrow \rho\alpha$, $\gamma \rightarrow P$ $(e\alpha + ec)$

for the 0.6 pct Csteel, $L \rightarrow \gamma$, $\gamma \rightarrow \rho\alpha$, $\gamma \rightarrow P$ $(e\alpha + ec)$

In the case of iron and 0.1 pct C steel (steel 1), the first phase to be formed is delta ferrite (δ). Some degrees above the solidus (S), steel goes through the peritectic transformation ($L + \delta \rightarrow \gamma$), which then, below the solidus, changes to the solid-state transformation ($\delta \rightarrow \gamma$).
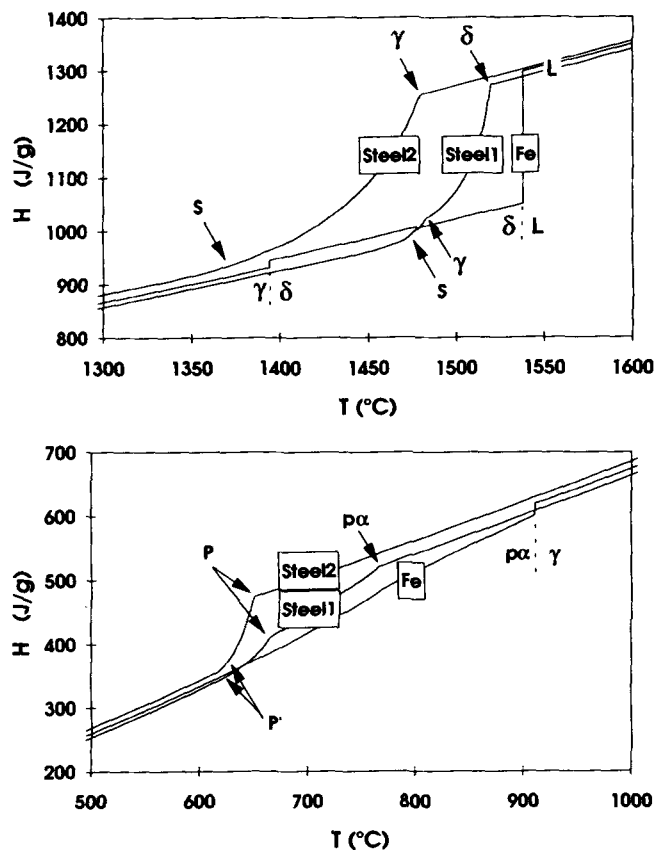

Fig. 3—Enthalpy of pure iron and steel, 1 pct Mn, 0.02 pct P, 0.3 pct Si containing 0.1 pct C (steel 1) or 0.6 pct C (steel 2) and cooled at a rate of $\dot{T}$ = 1 °C/s. Symbols are L = liquid, δ = delta ferrite, γ = austenite, S = solidus temperature, $\rho\alpha$ = proeutectoid ferrite, P = pearlite, and P' = end of pearlite reaction.

In the case of the 0.6 pct C (steel 2), the solidification is totally austenitic. At lower temperatures, austenite decomposes in both steels to proeutectoid ferrite ($\rho\alpha$) and, later, also to pearlite (P).

Figure 3 shows that in steel 1, not only the formation of delta ferrite but also the formation of austenite (γ), proeutectoid ferrite ($\rho\alpha$), and pearlite (P) accelerates the heat release. In steel 2, the heat release during the pearlite reaction is quite effective due to the quite narrow temperature range T^P to $T^{P'}$ of the austenite decomposition. Note that in the case of steel 1, this range is much wider, from $T^{\rho\alpha}$ to $T^{P'}$.

Figure 4 shows that proeutectoid ferrite ($\rho\alpha$) increases the specific heat of pure iron. At the Curie point of pure iron (770 °C), the specific heat increases sharply and then decreases smoothly as the temperature decreases. In steel 1, specific heat increases due to the formation of proeutetoid ferrite and pearlite. The increase is weaker than in pure iron because of the gradually increasing ferrite fraction during the $\gamma \rightarrow \rho\alpha$ transformation. In the case of steel 2, the strong increase of the specific heat due to the pearlite formation can be explained by the narrow temperature range of austenite decomposition.

The cooling rate is also an important parameter. While affecting the kinetics of phase transformations, it also affects the thermophysical properties of the alloy. As an
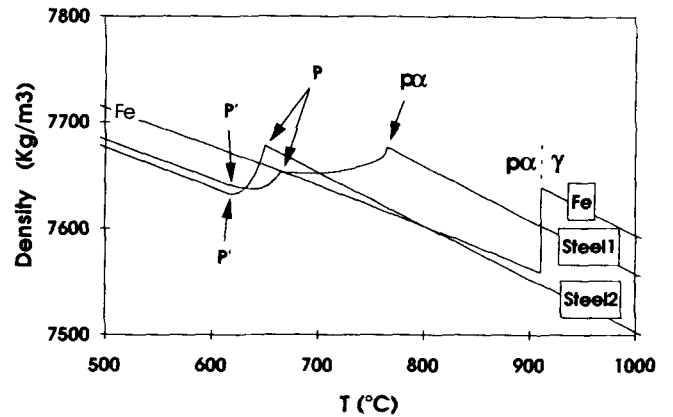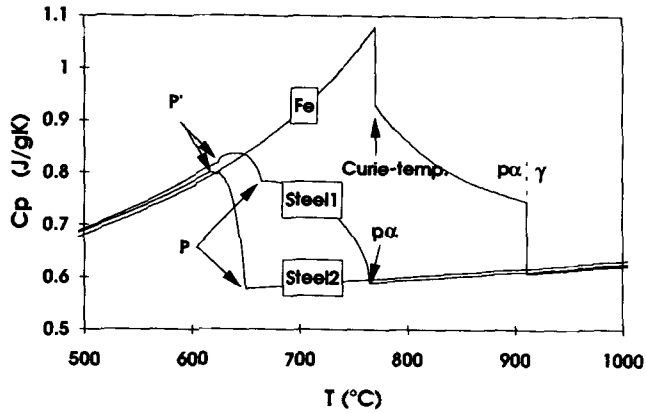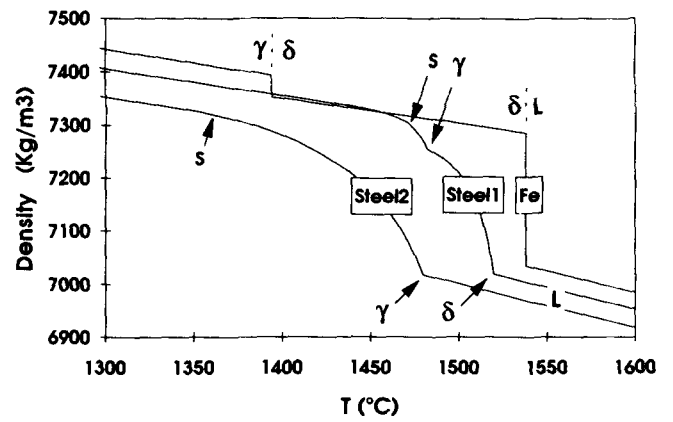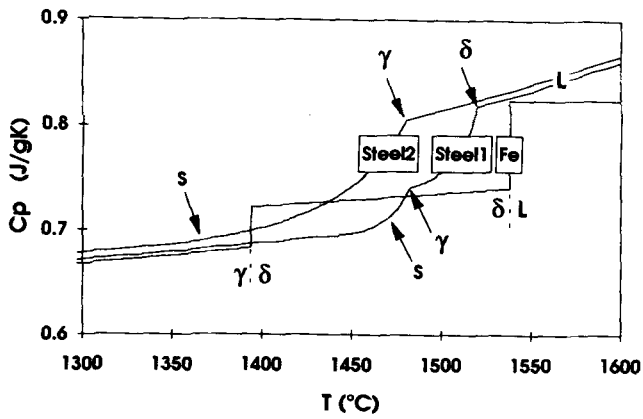
Fig. 4—Specific heat of pure iron and steel, 1 pct Mn, 0.02 pct P, 0.3 pct Si containing 0.1 pct C (steel 1) or 0.6 pct C (steel 2) and cooled at a rate of $T = 1$ °C/s. Symbols are L = liquid, δ = delta ferrite, γ = austenite, S = solidus temperature, $p\alpha$ = proeutectoid ferrite, P = pearlite, and P' = end of pearlite reaction.

Fig. 6—Density of pure iron and steel, 1 pct Mn, 0.02 pct P, 0.3 pct Si containing 0.1 pct C (steel 1) or 0.6 pct C (steel 2) and cooled at a rate of $T = 1$ °C/s. Symbols are L = liquid, δ = delta ferrite, γ = austenite, S = solidus temperature, $p\alpha$ = proeutectoid ferrite, P = pearlite, and P' = end of pearlite reaction.
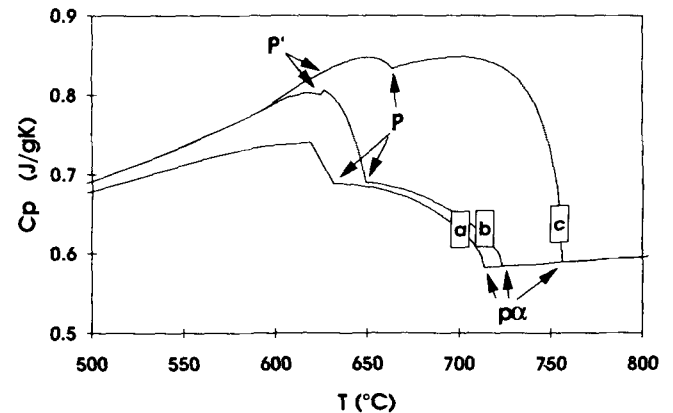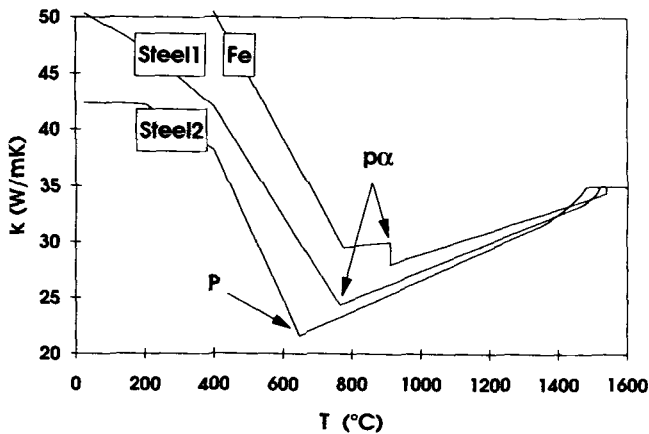

Fig. 5—Thermal conductivity of pure iron and steel 1 pct Mn, 0.02 pct P, 0.3 pct Si containing 0.1 pct C (steel 1) and 0.6 pct C (steel 2) and cooled at a rate of $T = 1$ °C/s. Symbols are: $p\alpha$ = proeutectoid ferrite and P = pearlite.

Fig. 7—Specific heat of steel, 0.2 pct C, 1 pct Mn, 0.02 pct P, 0.3 pct Si cooled at a rates of (a) $T = 10$ °C/s, (b) $T = 0.1$ °C/s, and (c) $T = 10$ °C/s at $T > 1000$ °C and $T = 0.1$ °C/s at $T < 1000$ °C. Symbols are $p\alpha$ = proeutectoid ferrite, P = pearlite, and P' = end of pearlite reaction.

example, Figure 7 shows the effect of cooling rate upon the specific heat at lower temperatures. As can be seen, a high cooling rate delays the formation of new phases (cases a and b). The cooling rate also affects the fractions of phases to be formed during phase transformations and, also in this way, the material properties. Note

also that a high cooling rate during solidification refines the grain size. This also affects the kinetics of the phase transformations and the material properties (case c in Figure 7).

Figure 8 shows the calculated latent heat values of solidification for the iron-carbon system and for a steel
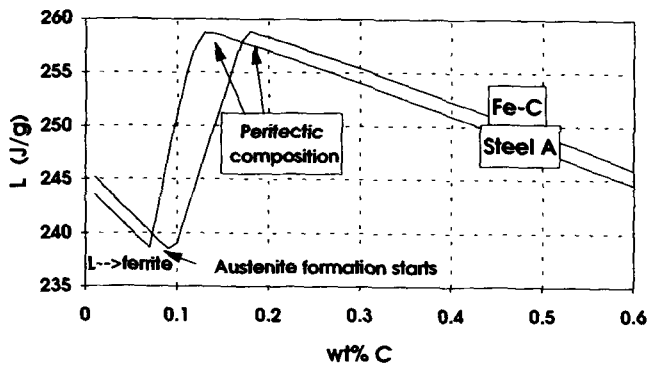
Fig. 8—Calculated latent heat of solidification as a function of carbon content for Fe-C system and for steel A: X pct C, 1 pct Mn, 0.02 pct P, and 0.3 pct Si, cooled at a rate of $T = 1$ °C/s.

grade A, 1 pct Mn, 0.02 pct P, 0.3 pct Si, as a function of carbon content. Up to about 0.1 pct C, the liquid solidifies fully to δ-ferrite and the latent heat decreases with increasing carbon content (or with decreasing solidus temperature). Above about 0.1 pct C, the steels solidify partly to austenite through the peritectic reaction and, with increasing austenite fraction, the latent heat increases. At the peritectic composition (for the Fe-C-system 0.17 pct C), the steel already solidifies fully to austenite (through the peritectic reaction). The latent heat is highest at the peritectic composition. Above the peritectic composition, the latent heat again decreases with increasing carbon content (or with decreasing solidus temperature).

The calculation package is now valid for carbon and low-alloyed steel grades and is under progress for stainless and alloyed steels. The development work of the calculation algorithms will also be continued. One question, for instance, is what the original austenite grain size is after solidification. Accurate data seem not to be available. Moreover, additional experimental CCT data will be used for the determination of the regression formulas in the ADC model, and more thermodynamic assessment data will be added to the database of the model package. More data on thermophysical properties are searched and comparisons between calculated values and experimental results will be continued. One future aim also involves connecting the calculation package iteratively to a heat-transfer model of continuous steel casting.

V. CONCLUSIONS

Algorithms and a computer software package for calculating thermophysical material properties of steels, taking into account the temperature, the cooling rate, and the composition, have been developed. The calcu-

lation algorithms are based on thermodynamic theory connected to thermodynamic assessment data, as well as on regression formulas of experimental data. The package is now valid for carbon and low-alloyed steel grades and is under progress for stainless and alloyed steels. Some comparisons between the calculated results and measured values were done and a good agreement was found,[1,2,3] but more comparisons are planned, especially on enthalpy and on enthalpy-related data, such as specific and latent heats. The development work of the calculation algorithms will also be continued.

REFERENCES

1. J. Miettinen: Metall. Trans. A, 1992, vol. 23A, pp. 1155-70.
2. J. Miettinen: Ph.D. Thesis, Helsinki University of Technology, Espoo, Finland, 1992.
3. J. Miettinen: Helsinki University of Technology, Espoo, Finland, unpublished research, 1994.
4. C. Wagner: Thermodynamics of Alloys, Addison-Wesley, Reading, MA, 1952.
5. C.H.P. Lupis and J.F. Elliott: Acta Metall., 1966, vol. 14, pp. 529-38.
6. S. Srikanth and K.T. Jacob: Metall. Trans. B, 1988, vol. 19B, pp. 269-75.
7. A.T. Dinsdale: CALPHAD, 1991, vol. 15, pp. 317-425.
8. W. Huang: Metall. Trans. A, 1991, vol. 22A, pp. 1911-20.
9. C. Qiu: Ph.D. Thesis, Royal Institute of Technology, Stockholm, 1993.
10. J.E. Lait, J.K. Brimacombe, and F. Weinberg: Ironmaking and Steelmaking, 1974, vol. 1, pp. 90-97.
11. E.A. Mizikar: Trans. TMS-AIME, 1967, vol. 239, pp. 1747-53.
12. I. Saucedo, J. Beech, and G.J. Davies: Met. Technol., 1982, vol. 9, pp. 282-91.
13. S. Louhenkilpi, E. Laitinen, and R. Nieminen: Metall. Trans. B, 1993, vol. 24B, pp. 685-93.
14. F. Richter: Die Wichtigsten Physikalischen Eigenschaften von 52 Eisenwerkstoffen, Verlag Stahleisen M.B.H., Dusseldorf, Germany, 1973.
15. F. Richter: Physikalischen Eigenschaften von Stählen un ihre Temperaturabhängigkeit, Verlag Stahleisen M.B.H., Dusseldorf, Germany, 1983.
16. C.D. Smithells: Metals Reference Book, 5th ed., Butterworth and Co. Ltd., London, 1976.
17. P.J. Wray: Proc. Modeling of Casting and Welding Processes, Rindge, NH, Aug. 3-8, 1980, H.D. Brody and D. Apelian, eds., TMS-AIME, Warrendale, PA, 1981, pp. 245-57.
18. A. Jablonka, K. Harste, and K. Schwerdtfeger: Steel Res., 1991, vol. 62, pp. 24-33.
19. C. Benedicks, N. Ericsson, and G. Ericsson: Arch. Eisenhüttenwes., 1930, vol. 3, p. 473.
20. A. Olsson: Scand. J. Metall., 1981, vol. 10, pp. 263-71.
21. A. Fernandez Guillermet and P. Gustafson: High Temp.-High Pressures, 1985, vol. 16, pp. 591-610.
22. P. Gustafson: Scand. J. Metall., 1985, vol. 14, pp. 259-67.